

# Role of longitudinal activity complexes for solar and stellar dynamos

Maarit J. Mantere<sup>1,2</sup>, Petri J. Käpylä<sup>1,3</sup>, Jaan Pelt<sup>4</sup>

<sup>1</sup>Department of Physics, PO Box 64, FI-00014 University of Helsinki, Finland

<sup>2</sup>Department of Information and Computer Science, Aalto University, PO Box 15400, FI-00076 Aalto, Finland

<sup>3</sup>Nordita, KTH Royal Institute of Technology and Stockholm University, Roslagstullsbacken 23, SE-10691 Stockholm, Sweden

<sup>4</sup>Tartu Observatory, Tõravere, 61602, Estonia

**Abstract.** In this paper we first discuss observational evidence of longitudinal concentrations of magnetic activity in the Sun and rapidly rotating late-type stars with outer convective envelopes. Scenarios arising from the idea of rotationally influenced anisotropic convective turbulence being the key physical process generating these structures are then presented and discussed - such effects include the turbulent dynamo mechanism, negative effective magnetic pressure instability (NEMPI) and hydrodynamical vortex instability. Finally, we discuss non-axisymmetric stellar mean-field dynamo models, the results obtained with them, and compare those with the observational information gathered up so far. We also present results from a pure  $\alpha^2$  mean-field dynamo model, which show that time-dependent behavior of the dynamo solutions can occur both in the form of an azimuthal dynamo wave and/or oscillatory behavior related to the alternating energy levels of the active longitudes.

**Keywords.** MHD – turbulence – Sun: magnetic fields – Stars: magnetic fields

---

## 1. Introduction

The spectroscopic time series obtained for rapidly rotating late-type stars, analyzed with Doppler imaging methods, have revealed huge high-latitude temperature anomalies unevenly distributed over the stellar longitudes. The analysis of photometric time series have in many cases confirmed the spectroscopic results, and allowed the follow-up of the evolution of the light curve minima for longer time intervals and with better time sampling. From these investigations it seems clear that in many stars the magnetic activity manifests itself as active longitude(s) that undergo apparently quite irregular phase jumps, sometimes called flip-flops, and drifts in the rotational frame of reference. In terms of dynamo theory, a change from the solar-type mostly axisymmetric and quite regular oscillatory solution to a non-axisymmetric non-stationary mode is expected to occur as the rotation rate is increasing.

Some of the phenomena related to these active longitudes can rather straightforwardly be understood using mean-field dynamo theory (see e.g. Krause & Rädler, 1980). The change from axi- to non-axisymmetric solutions with increasing rotation rate, for instance, is a prediction dating back to kinematic linear dynamo solutions, that has been later confirmed by more complex non-linear modeling. Time-dependent solutions, with the angular frequency of the non-axisymmetric modes being different from the axisymmetric mode and stellar rotation constituting an azimuthal dynamo wave, have also been recognized as common linearly preferred and non-linearly stable solutions to the dynamo

equations. Understanding and explaining the flip-flops has remained a prominent challenge both observationally and theoretically. Photometry and Doppler imaging naturally do not give the information of the polarity of the spots on the active longitudes. Therefore it has been impossible to differentiate whether the phase jumps are related only to the alternation of the magnetic energy levels of the spots, or are polarity changes also related to the phenomenon. Only very recently such observational data has become available; as will be discussed in Sect. 2.2, the analysis and interpretation of the data is far from straightforward, and clear conclusions are still missing. Theoretically, oscillatory solutions are more generally associated with  $\alpha\Omega$  dynamo solutions, where differential rotation is dominating the field generation over the  $\alpha$  effect. In the rapid rotation regime, however, differential rotation is expected to be suppressed. It has remained challenging to find oscillatory solutions of pure  $\alpha^2$  type, although it has been known since the kinematic calculations that such solutions are possible. Recently, more results of oscillatory  $\alpha^2$  dynamo solutions have emerged, and in this paper we also demonstrate one such model in Sect. 3.4.1.

One of the most puzzling results related to the spectropolarimetric observations, yielding the surface magnetic field strength and orientation with the surface temperature distribution, is that very seldom clear anticorrelation between the magnetic field strength and temperature (see e.g. Kochukhov *et al.* 2013 and references therein), expected from the sunspot analogy, is found. From theoretical point of view, it is, indeed, quite poorly understood how the dynamo-generated sub-surface fields transform themselves into sun- or starspots, and whether the same mechanisms are actually at play in all the objects under study. The sunspot sizes, for instance, are on average much smaller than the scale of the toroidal magnetic field belt that they emerge from according to dynamo theory - this is to be contrasted to the starspots that have surface areas large enough to be regarded as global large-scale phenomena as the dynamo-generated field itself.

The rather widely accepted paradigm of sun- and starspot formation is the so called rising flux tube model (see e.g. Choudhuri & Gilman, 1987), according to which strong magnetic flux is generated and stored in the tachoclinic shear layer just beneath the convectively unstable region. The magnetic field becomes unstable and rises to the surface in the form of thin flux tubes, due to buoyancy force, during which process it becomes only weakly affected by the turbulent motions in the convection zone. Closely related to this paradigm is the flux transport dynamo scenario (see e.g. Dikpati & Charbonneau, 1999), furthermore relying on the inductive effect due to sunspot decay near the solar surface (Babcock-Leighton effect) accompanied with a conveyor belt provided by meridional circulation, reviewed by Choudhuri (2013) in these proceedings. Again, convective turbulence plays a negligible role in the flux transport model, even the turbulent diffusion being reduced significantly from the simple estimates e.g. from mixing length theory. In this paper, we concentrate more on the turbulent dynamo picture (see e.g. Brandenburg & Subramanian, 2005; Pipin, 2013 in these proceedings), which relies on the idea of magnetic field generation both by rotationally affected anisotropic convective turbulence and large-scale flows and non-uniformities in the stellar rotation profile. Sun- and starspot formation mechanisms directly related to turbulence effects include the negative effective magnetic pressure instability (NEMPI) and hydrodynamic vortex instability, both of which are also reviewed in this manuscript. In the context of NEMPI from turbulent convection, we also refer to the paper by Käpylä *et al.* (2013) in these proceedings.

Next, we give a short review of stellar dynamo models capable of solving for non-axisymmetric modes, and the results obtained with them in Sect. 3.4. We note that results in this field are much less abundant than in the solar case, where axisymmetric

(in two dimensions) modeling is adequate. Finally, a summary and main conclusions are presented in Sect. 4.

## 2. Observational studies of active longitudes

The study of longitudinal concentrations of magnetic activity started with the accumulation of data of the distribution of solar activity tracers on its surface (systematic sunspot observations, solar flares, and so on). It was realized that they do not occur completely randomly over the longitudes, but 'hot spots' or 'activity nests' surviving over several years, maximally over the whole solar cycle, in which the major sunspots and flares were accumulating over time, frequently occur. The first tool was to create family trees (time-longitude diagrams) of the activity complexes, aiming at following the pattern they formed over time on the solar surface - using this technique it soon became evident that the hot spots were not always moving with the same rotation rate as the solar surface, nor the Northern vs Southern activity complexes as a synchronized structure (see e.g. Bai, 1987 and references therein). Evidently, something interesting was going on, which ignited an intensive study of the phenomenon with sophisticated time series analysis tools.

### 2.1. *Is the solar magnetic field axisymmetric?*

Several parametric and non-parametric time series analysis methods have been used to analyze the distribution of sunspots and solar flares over the past few decades. As the family tree analysis had already revealed that the rotation period of the hot spots was unlikely to match with the surface rotation rate, the first hypothesis was to assume that it does not, and try to find the most suitable rotation period that produces the most uneven distribution (i.e. the strongest clustering) of the activity traces over the solar longitudes. Again, South and North seemed to be decoupled, the other natural hypothesis being to keep them separate in the analysis. Very often the term 'active longitude' is used, in a strict sense meaning, that at any latitude, being it Northern or Southern, the activity should manifest itself at the same longitude. This definition does not make much sense in any observational case - the solar hemispheres behave in a decoupled manner, and usually only a fraction of the whole latitudinal extent is seen of other stars. In the dynamo models, however, the solutions indeed form a coherent longitudinal structure over the whole latitudinal range, fulfilling the definition of an active longitude. Nevertheless, the paradigm of active longitudes has strongly influenced the discussion and analysis methods of solar activity tracers; very often bimodal distributions are the ones searched for, i.e. the distributions producing the strongest two-peaked distributions are normally ranked to be the most desirable. Even if not, the statistical significance of longitudinal clustering of *any* number of peaks in the histograms has been found to be very low. Furthermore, the best period calculated for the whole data set might not represent well both hemispheres, nor be the best if the data was divided into shorter intervals. This has led to the overall conclusion that the non-axisymmetric component, at least the one that would be rigidly rotating, of the solar dynamo must be very weak and apparently dynamically changing over time.

It is well known that the solar convection zone is differentially rotating so that at the surface, the pole rotates slower than the equator. The next hypothesis adopted was to postulate, that the surface distribution of activity traces becomes affected by this rotation pattern. This essentially means that time series analysis methods allowing for one free parameter more to be fitted, namely the amount and direction of the surface differential rotation pattern, were developed. Again, using the maximal clustering as

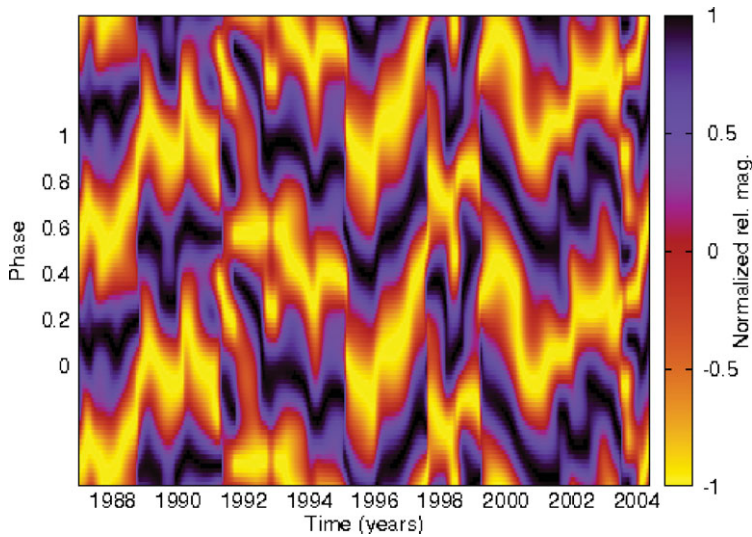


**Figure 1.** Photometric lightcurve of FK Comae Berenices for 1987–2004 analyzed with the Carrier Fit method (Pelt *et al.*, 2011; see also Hackman *et al.*, 2012b). Number of model harmonics used is  $K = 3$ , number of modulation harmonics  $L = 20$ , modulation period of 9000 days, and carrier period  $P_0 = 2.4002466d$ .

the measure of the statistical significance of the solution, it was claimed (Berdyugina & Usoskin, 2003; Usoskin *et al.*, 2005; Berdyugina *et al.*, 2006) that a persistent system of active longitudes, comprising roughly 10% of the total number of sunspots, was present in the Sun, made visible by the ‘passing’ sunspot distribution on the surface experiencing differential rotation. The existence of this stroboscopic effect was put under doubt by the following investigations (Pelt *et al.* 2005; 2006), which showed that even the differentially rotating constructions produced longitudinal distributions that had a significance level comparable to a statistical fluctuation. On the other hand, it was shown (Pelt *et al.* 2010) that the sunspot distribution, and therefore the magnetic field structure from which it originates, is indeed affected by differential rotation. Moreover, it was shown that nonparametric methods can be used to determine the coherence time of the non-axisymmetric structures; the average coherence time was estimated to be roughly 10–15 Carrington rotations.

As a conclusion, one might say that a weak non-axisymmetric component of the solar magnetic field exists, and is affected by the differential rotation of the solar convection zone. Due to its weakness and dynamical nature, it is very hard to quantify it even with the best statistical tools and despite of the long time span of the sunspot data. Most of the solar dynamo models work under the assumption of axisymmetry, which seems to be safe, taken what is said above. Here we note, however, that also non-axisymmetric solar dynamo models have been developed (e.g. Moss, 1999), where the excitation of a sub-dominant non-axisymmetric magnetic field modes has been seen. These models are kinematic, i.e. no back-reaction of the magnetic field on the velocity field is taken into account. Therefore, these models do not properly address the dynamical significance of these modes.

## 2.2. Rapidly rotating late-type stars

Direct observational ways to detect and characterize spots and their longitudinal distributions on stellar surfaces include photometric lightcurve analysis, spectroscopic Doppler

imaging, and spectropolarimetric Zeeman-Doppler imaging. Observational result that has had the strongest impact on the discussion of active longitudes came from the analysis of the photometry of FK Comae Berenices by Jetsu *et al.* (1993). By analyzing 25 years of photometry, two active longitudes, roughly 180 degrees apart were found. The activity was seen to abruptly switch from one longitude to the other, the jump detected three times in the data analysed. This phenomenon was given the name 'flip-flop'; analysis of lightcurves of other rapidly rotating late-type stars (e.g. Berdyugina & Tuominen, 1998) soon established the fact that flip-flops are a common phenomenon related to the stellar cycle. Doppler imaging results, yielding the surface temperature distribution, confirmed the photometric results (e.g. Korhonen *et al.*, 2004 and references therein), although with poorer time sampling.

When these stars were followed up for a longer time span, it first became evident that the active longitude system is not stable in the rotational frame of reference of the stellar surface, i.e. the non-axisymmetric system either formed straight, inclined, railroads either upwards and downwards on the phase-time plots (e.g. Berdyugina & Tuominen, 1998), or even more complicated patterns of railroads with changing inclination (Jetsu *et al.*, 1999 for V 1794 Cyg), sinusoidal paths (Berdyugina *et al.* 2002 for LQ Hya; Berdyugina & Järvinen, 2005 for AB Doradus) and so on. This revealed the other type of time-dependent behavior of the active longitudes - the non-axisymmetric system rotates with a different speed than the star itself, and this rotation period actually changes over time. This does not sound completely unfamiliar, as the solar hot spots are known to exhibit the same behavior. Secondly, the longer the stars were followed, the less periodic and regular the flip-flop events appeared. To illustrate the situation for FK Comae Berenices, we have re-analysed its photometry for the years 1987-2004 (Oláh *et al.*, 2006; Korhonen *et al.*, 2007) with the Carrier Fit (CF) method (Pelt *et al.*, 2011), see Fig. 1. Here, we have used the well-known photometric rotation period of  $P_0 \approx 2.4$ d as the carrier in our analysis, and computed the continuous longitudinal distribution of spots, appearing as dark regions in the plot, on the star. One of the 'well-behaved' flip-flop events reported by Jetsu *et al.* (1993) is visible during the first 3 years of the data. Since then, at least four other flip-flop type events have occurred, but the time intervals between them is clearly not regular. Moreover, railroad patterns (tracks tilted up- and downwards) appear in the data since 1995 indicating that the non-axisymmetric structure does no longer rotate with the photometric rotation period, but can lag behind or speed up with respect to it. This photometric analysis is in rough agreement with Doppler imaging results, see Korhonen *et al.* (2004). For a more detailed analysis of the phase jumps we refer to Oláh *et al.* (2006) and Hackman *et al.* (2013).

The railroad pattern is especially clear and persistent in the case of the RS CVn binary system's primary giant component II Peg (see Fig. 2; Lindborg *et al.*, 2013). Instead of two active longitudes, in this star we see the dominance of one dark region, with sporadic appearance of a secondary minimum roughly 180 degrees apart from the primary one (see Berdyugina *et al.*, 1998, 1999; Lindborg *et al.*, 2011; Hackman *et al.*, 2012 for surface images). The dominance of the other active longitude could be thought to arise from the binarity, but the situation is far from being that simple. Namely, the CF analysis reveals a persistent downward trend in the phase-time diagram over most of the timespan, indicating that the spotted structure on a single active longitude is rotating faster than the star itself. This is a very peculiar finding, especially reflected upon the fact that in the system of close binary stars, the orbital period becomes synchronized. It is possible that the synchronization of the orbit has not yet fully occurred, but then the dominance of one active longitude due to binarity and synchronism appears invalid. Moreover, the systematic trend seems to break down towards the end of the data set. During this epoch,

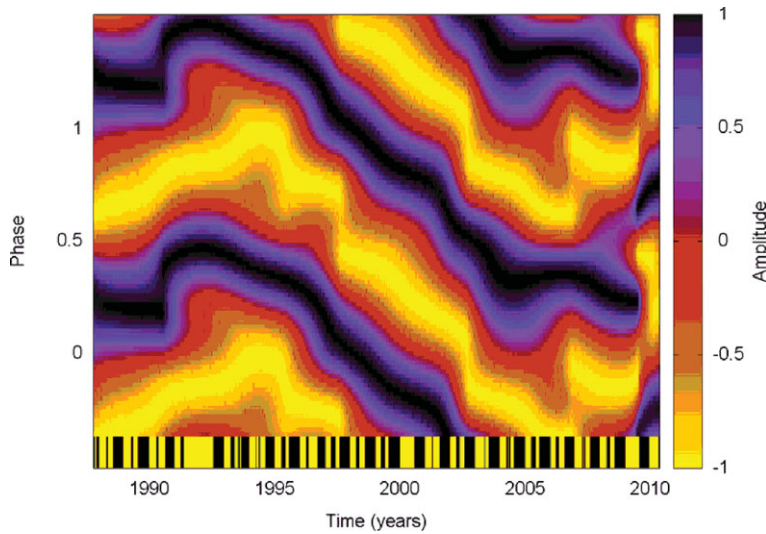


**Figure 2.** Photometric lightcurve of II Peg for 1988-2010 analyzed with the Carrier Fit method (Pelt *et al.*, 2011). Number of model harmonics used is  $K = 3$ , number of modulation harmonics  $L = 5$ , modulation period of 10000 days, and Carrier period  $P_0 = 6.724333d$ .

Doppler imaging (Hackman *et al.*, 2012) and Zeeman Doppler imaging (Kochukhov *et al.*, 2013) suggest that the magnetic activity level of the star is attaining a minimum. Generally, the analysis of photometry is in good agreement with the Doppler imaging results (see e.g. Hackman *et al.*, 2011, Lindborg *et al.*, 2013), although the decreasing trend in the spot intensity is not visible in Fig. 2 due to the adopted normalization in our plot (each stripe is normalized with its extrema to enhance the drift pattern during the epoch of weaker spots).

Comparing photometry and Doppler images to magnetic maps (Kochukhov *et al.*, 2013) brings further complications into the interpretation, although it has to be kept in mind that magnetic maps exist only for the lower state activity epoch - magnetic maps clearly show two active longitudes of different polarities virtually at all times the star has been imaged, which undergo polarity changes without any signs of flip-flop occurring with the other methods. Only exception to this are the most recent observing seasons (2008-2010), during which a polarity change might be associated with the abrupt-looking phase behavior seen also in Fig. 2.

### 3. Explanations in the framework of turbulent dynamo theory

To understand the gradually building up observational picture, theory should address at least the following two fundamental issues: Firstly, the models should be capable of reproducing the transition from oscillatory, mostly axisymmetric dynamo in the  $\alpha\Omega$  regime (differential rotation dominating over the effect of convective turbulence) into the dominantly non-axisymmetric dynamo in the pure  $\alpha^2$  regime (field generation presumably taking place with negligible differential rotation) when the rotation rate of the star is increased. The usage of 'presumably' here refers to the fact that we do not actually yet observationally know the internal rotation profiles for other stars than the Sun; the only information comes from modeling (see e.g. Kitchatinov & Rüdiger, 1999). Secondly, what is the relation of the large-scale dynamo-generated magnetic field and the sun- and starspots themselves, and how does one form spots from the underlying dynamo field?

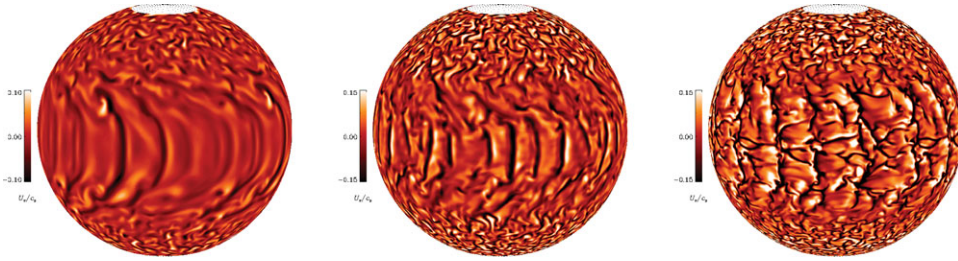


**Figure 3.** Radial velocity  $U_r$  from three simulations of rapidly rotating turbulent convection with density contrasts of 5 (left), 30 (middle), and 100 (right) in spherical wedge geometry. Adapted from Käpylä *et al.* (2011b).

Both of these issues have been addressed from the point of view of a turbulent dynamo, which viewpoint is adopted in this paper; the competing theory of the transport of rising flux tubes is discussed in length by Choudhuri (2013) in these proceedings. According to the theory of a turbulent dynamo (for an extensive review, see Brandenburg & Subramanian, 2005), the dynamo instability itself is affected by the presence of turbulence so that a collective inductive action plus an enhanced diffusion is caused by turbulence effects; as the convection zone is turbulent throughout, these effects are distributed over the total extent of it - sometimes the term distributed dynamo is used to denote the turbulent dynamo process. Turbulence effects can also lead to certain types of instabilities, that have been shown to result in the formation of magnetic field concentrations or global-scale temperature anomalies. On the other hand, structure formation in convectively turbulent flow can occur via other, less specified, routes, which provides us a starting point for the theoretical discussion.

### 3.1. Spontaneous formation of magnetic field concentrations in turbulent convection simulations

Direct numerical solutions of magnetized convection have reached a level of sophistication where the formation of flux concentrations can be self-consistently modeled. Global and semi-global simulations of rapidly rotating convection exhibit non-axisymmetric convection at low latitudes when the magnetic field is weak or absent (e.g. Brown *et al.* 2008; Käpylä *et al.* 2011b; Augustson *et al.* 2012, see the leftmost panel of Fig. 3). This behavior is most prominent near the onset of convection. Furthermore, increasing density stratification seems to suppress the non-axisymmetric modes (Käpylä *et al.* 2011b, compare the middle and rightmost panel of Fig. 3 to the leftmost one). However, as the magnetic fields due to dynamo action become dynamically important, the non-axisymmetric convection patterns disappear and the large-scale magnetic fields are also mostly axisymmetric (e.g. Brown *et al.* 2011); see, however, Miesch *et al.* (2013) in these proceedings.

Another line of study concerns local simulations where some sort of magnetic field is imposed or advected into the system. In these cases turbulent convection can rearrange the magnetic field self-consistently into concentrations in contrast to the sunspot simulations of Rempel *et al.* (2009) where the spots are the result of an imposed magnetic field structure. The outcomes of these models are either large-scale magnetic structures (e.g. Tao *et al.*, 1998), or can resemble pores (Kitiashvili *et al.*, 2010) or even bipolar regions in the Sun (Stein & Nordlund, 2012). The exact mechanism responsible for the flux concentrations in these cases is not yet certain.

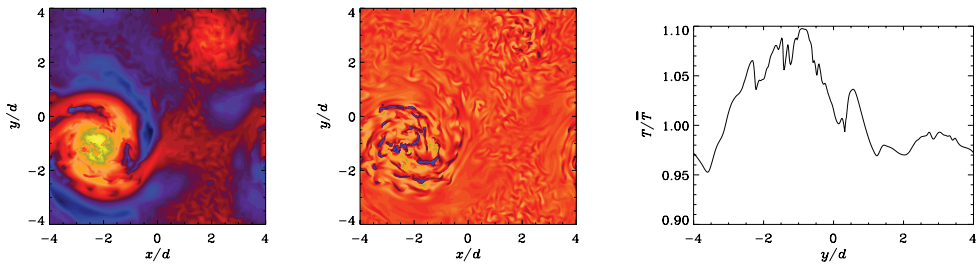


**Figure 4.** Large-scale vortices in rapidly rotating turbulent convection in Cartesian geometry. Left and middle panels show the temperature and vertical velocity, respectively, near the surface of the convectively unstable region. The right panel shows a cut of the temperature through the warm spot in the lower left corner of the left panel. Adapted from Mantere *et al.* (2011).

### 3.2. NEMPI

A possible mechanism for generating flux concentrations that ultimately lead to the formation of sun- and starspots is due to a negative contribution of turbulence to the effective magnetic pressure (e.g. Kleeorin *et al.* 1990; Rogachevskii & Kleeorin 2007), a.k.a. the negative effective magnetic pressure instability (NEMPI). This effect can form flux concentrations even from uniform, sub-equipartition, magnetic fields.

Mean-field models and direct numerical simulations of forced turbulence have established that the negative effect exists (e.g. Brandenburg *et al.* 2010, 2012), and the instability itself has been detected in direct numerical simulations (DNS) of forced turbulence (Brandenburg *et al.* 2011). A negative effect on magnetic pressure has also been found for convection (Käpylä *et al.* 2012a) but no NEMPI has been detected so far (see, however, Käpylä *et al.* (2013) in these proceedings).

### 3.3. Large-scale hydrodynamic vortex instability

The apparent uncorrelation of magnetic fields and temperature anomalies in Zeeman–Doppler maps of stars is a puzzling feature, which may be attributable to the limited spatial resolution of the current ZDI maps (see discussion in Kochukhov *et al.*, 2012), or explained with a new mechanism by which starspots can be generated without a correlation of magnetic fields and temperature. The latter possibility has been recently considered on the basis of results from local *hydrodynamic* simulations of rapidly rotating turbulent convection (Käpylä *et al.* 2011a; Mantere *et al.* 2011). It turns out that when certain threshold values of the Reynolds and Coriolis numbers, describing the effects of molecular viscosity and rotation on the flow, are exceeded, large-scale vortices appear in the system. When rotation is gradually increased, cool anti-clockwise vortices appear first. For more rapid rotation also warm clockwise cyclones appear (see Fig. 4). The temperature anomaly in the cyclones is at least ten per cent of the surface temperature which is similar to the spots seen in Doppler images of rapidly rotating stars. Similar vortices have not yet been found in global or semi-global simulations. A probable reason is too low resolution achievable at the moment. Furthermore, the vortices also seem to disappear in simulations where a magnetic dynamo is present (Käpylä *et al.* 2013a). Currently it is unclear whether the cyclones can coexist with strong magnetic fields.

### 3.4. Non-axisymmetric mean-field dynamos

Modeling of the solar dynamo is at the verge of becoming accessible by DNS (Ghizaru *et al.* 2010), the first solar-type solutions having been obtained from such models (Käpylä *et al.*, 2012c). Such models, however, are computationally expensive, and mean-field approach still has clear advantages in this respect. The solar mean-field models usually



work under the assumption of axisymmetry, reducing the problem into two spatial dimensions, whereas it is obvious from observations that this assumption is not valid for the more rapidly rotating stars with dominantly non-axisymmetric surface temperature and magnetic field configurations. Non-axisymmetric models necessarily solve for the azimuthal dependence of the physical quantities, either on a finite-difference or -volume grid, or using spherical harmonic decomposition and Fourier transform.

The non-axisymmetric solutions to the kinematic  $\alpha^2$  equations in simple setups were computed already decades ago (see e.g. Rädler, 1975; Krause & Rädler, 1980), providing more or less all the essential properties of the solutions: when rotation rate is increased enough, the preferentially excited modes are the non-axisymmetric ones, typically representing quadrupolar symmetry (S1). The solutions are usually non-oscillatory, but still time-dependent, as the modes migrate either east- or westward. The nonlinear, sometimes even dynamical, models developed since the 1990's (see e.g. Moss et al. 1995; Küker & Rüdiger 1999) have shown that also antisymmetric dipolar solutions (A1) can appear as the nonlinearly stable solutions (Tuominen *et al.* 2002). In this type of a solution, two high-latitude spots of opposite polarities in the same hemisphere are generated, in agreement with what is observed e.g. in II Peg (e.g. Kochukhov *et al.*, 2013). Despite of the azimuthal dynamo wave generated by the east- or westward migration of the non-axisymmetric modes, the solutions reported have been non-oscillatory, therefore providing no explanation for the flip-flop type phase jumps.

In search for oscillatory solutions, one approach has been to include small amounts of differential rotation into the models (see e.g. Elstner & Korhonen, 2005), essentially meaning that the dynamo models are of  $\alpha^2\Omega$  type, where differential rotation is present, but is subdominant in the magnetig field generation. In this way, mixed solutions with an oscillatory axisymmetric mode and a stable non-axisymmetric one provide flip-flop type oscillatory behavior. On the other hand, it has been known since a long time that pure  $\alpha^2$  dynamos do have oscillatory solutions (see e.g. Baryshnikova & Shukurov, 1987; Bräuer & Rädler, 1987). In fact, only in the case of the  $\alpha$  effect being purely homogeneous and the system unbounded, the solutions are purely non-oscillatory. Recently, oscillatory  $\alpha^2$  solutions have been found in the spherical forced turbulence simulations of Mitra *et al.* (2010) and in local Cartesian simulations of turbulent convection (Käpylä *et al.*, 2013a). In the next subsection, we illustrate the possibility of oscillatory non-axisymmetric  $\alpha^2$  solutions in a simple mean-field dynamo model.

#### 3.4.1. Simple $\alpha^2$ dynamo model

We solve the mean-field induction equation in three dimensions using spherical polar coordinates  $(r, \theta, \phi)$ . The domain is a wedge spanning the latitude range  $(6^\circ, 174^\circ)$ , radius 0.6, 1.0 and the full azimuthal extent. The equation is solved with the PENCIL CODE† using a mesh  $32 \times 64 \times 128$ ; the spatial discretization in spherical polar coordinates does not allow us to explore the full latitudinal extent, as the time step decreases strongly close to the pole. The  $\alpha$  effect has a uniform radial profile, and  $\cos\theta$  dependence, obtaining maxima at the poles. The boundary conditions applied for the magnetic field, in terms of the vector potential that is solved for, are those of a perfect conductor at the lower radial and latitudinal boundaries, and normal-field conditions are applied at the top radial boundary:

$$\frac{\partial A_r}{\partial r} = A_\theta = A_\phi = 0 \quad (r = r_1), \quad (3.1)$$

† <http://pencil-code.googlecode.com/>

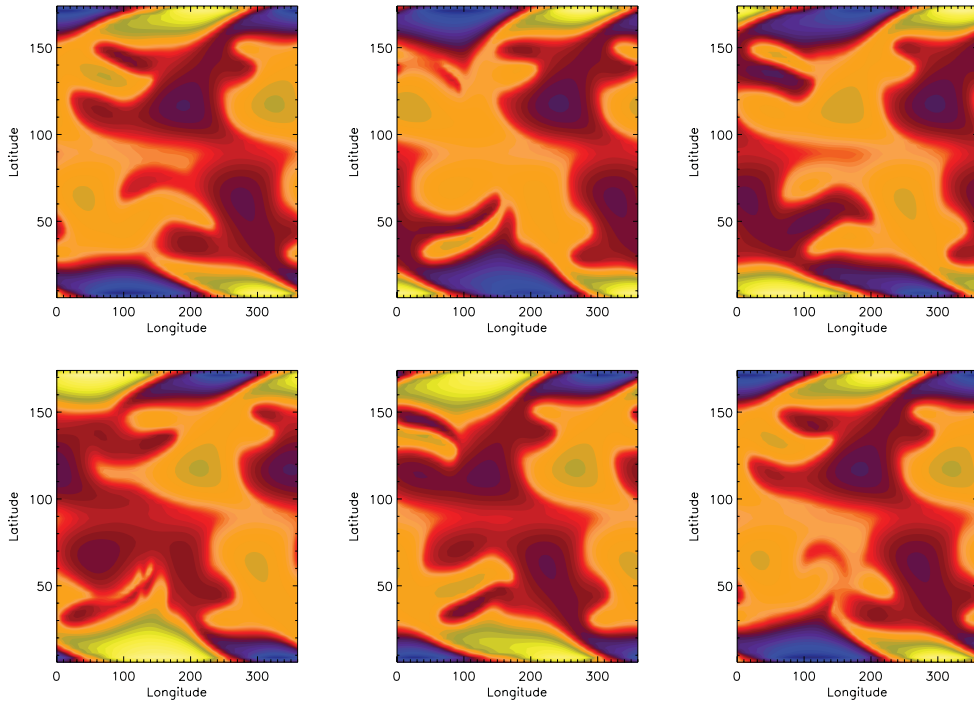


**Figure 5.** Radial magnetic field at the surface for six different times,  $t/\tau=(4.17,4.28,4.39,4.50,4.61,4.72)$  of the oscillation cycle of a solution with  $C_\alpha=5 \times 10^3$ .

$$A_r = 0, \frac{\partial A_\theta}{\partial r} = -\frac{A_\theta}{r}, \frac{\partial A_\phi}{\partial r} = -\frac{A_\phi}{r} \quad (r = r_3), \tag{3.2}$$

$$A_r = \frac{\partial A_\theta}{\partial \theta} = A_\phi = 0 \quad (\theta = \theta_1, \theta_2). \tag{3.3}$$

Azimuthal boundaries are treated as periodic. As a nonlinearity, a simple algebraic  $\alpha$ -quenching is used.

We perform calculations with varying strength of the  $\alpha$ -effect, spatially constant turbulent diffusion, and time being measured in diffusion times,  $\tau = d^2/\eta$ , where  $d$  is the depth of the convection zone. The strength of the  $\alpha$  effect is measured by the quantity  $C_\alpha = \alpha_0 R/\eta$ , where  $\alpha_0$  is varied. The critical  $C_\alpha$  above which growing solutions are obtained is roughly 50. A regime of axisymmetric oscillatory solutions of antisymmetric type is seen up to  $C_\alpha \approx 10^3$ . With larger values, the excited solutions become dominantly non-axisymmetric, and show eastward migration. The solutions are otherwise non-oscillatory. When  $\alpha$  effect is ramped up further, the solutions change into oscillatory ones. Time evolution of the radial field at the surface during one cycle of such a calculation is shown in Fig. 5, and magnetic energy densities for different magnetic field components in Fig. 6. The oscillation seen in the magnetic field energy densities is clearly related to the interchange of the magnetic field strength of spots with different polarities. Interestingly, the migration period of eastward drift equals the cycle length.

### 4. Conclusions

In this paper we have discussed observations and theory of longitudinal concentrations of solar and stellar activity tracers. While the solar magnetic field is dominantly

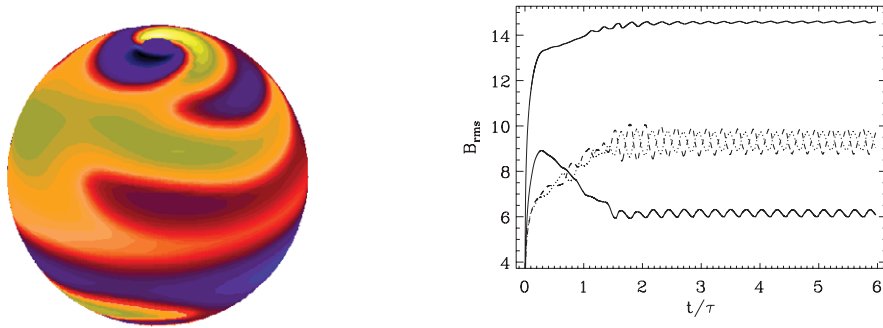


**Figure 6.** Left: snapshot of the radial magnetic field at the surface for  $t/\tau=4.39$  in spherical projection. Right: magnetic energy density of the different components (total –thick solid, radial – thin solid, latitudinal – dotted, azimuthal – dashed).

axisymmetric, non-axisymmetric modes dominate the magnetic fields of rapid rotators. The greatest challenges in the observational frontier include understanding the uncorrelation of temperature anomalies from magnetic field strength in ZDI, and determining whether and how the flip-flops and phase jumps relate to stellar activity cycles. Theoretically the most challenging task consists of explaining how the global dynamo-generated field transforms itself into sun- and starspots, and whether the mechanism is the same in all stars independent of the rotation rate.

### Acknowledgements

The computations were performed on the facilities hosted by the CSC – IT Center for Science in Espoo, Finland, which are financed by the Finnish ministry of education. We acknowledge financial support from the Academy of Finland grant Nos. 136189, 140970 (PJK), 218159 and 141017 (MJM), and the University of Helsinki research project ‘Active Suns’. MJM and PJK thank NORDITA for hospitality during their visits.

### References

- Augustson, K. C., Brown, B. P., Brun, A. S., Miesch, M. S., & Toomre, J. 2012, *ApJ*, 756, 169  
 Bai, T., 1987, *ApJ*, 314, 795  
 Baryshnikova, Iu & Shukurov, A., 1987, *AN*, 308, 89  
 Berdyugina, S. V., & Tuominen, I. 1998, *A&A*, 336, L25  
 Berdyugina, S. V., & Usoskin, I. G. 2003, *A&A*, 405, 1121  
 Berdyugina, S. V. & Järvinen, S. P., 2005, *AN*, 326, 283  
 Berdyugina, S. V., Berdyugin, A. V., Ilyin, I., & Tuominen, I. 1998, *A&A*, 340, 437  
 Berdyugina, S. V., Berdyugin, A. V., Ilyin, I., & Tuominen, I. 1999, *A&A*, 350, 626  
 Berdyugina, S. V., Pelt, J. & Tuominen, I. 2002, *A&A*, 394, 505  
 Berdyugina, S. V., Moss, D., Sokoloff, D., & Usoskin, I. G. 2006, *A&A*, 445, 703  
 Brandenburg, A. & Subramanian, K. 2005, *Phys. Rep.*, 417, 1  
 Brandenburg, A., Kleeorin, N. & Rogachevskii, I. 2010, *Astron. Nachr.*, 331, 5  
 Brandenburg, A., Kemel, K., Kleeorin, N., Mitra, Dhruvadyta & Rogachevskii, I. 2011, *ApJ*, 740, L50  
 Brandenburg, A., Kemel, K., Kleeorin, N. & Rogachevskii, I. 2012, *ApJ*, 749, 179  
 Brown, B. P., Browning, M. K., Brun, A. S., Miesch, M. S., & Toomre, J. 2008, *ApJ*, 689, 1354  
 Brown, B. P., Miesch, M. S., Browning, M. K., Brun, A. S., & Toomre, J. 2011, *ApJ*, 731, 69  
 Bräuer, H.-J. & Rädler, K.-H., 1987, *AN*, 308, 101  
 Choudhuri, A. R. & Gilman, P. A., 1987, *ApJ*, 316, 788  
 Dikpati, M. & Charbonneau, P., 1999, *ApJ*, 518, 508

- Elstner, D. & Korhonen, H., 2005, *AN*, 326, 278
- Ghizaru, M., Charbonneau, P., & Smolarkiewicz, P. K., 2010, *ApJL*, 715, 133
- Hackman, T., Mantere, M. J., Jetsu, L., Ilyin, I., Kajatkari, P., Kochukhov, O., Lehtinen, J., Lindborg, M., Piskunov, N., & Tuominen, I., 2011, *AN*, 332, 859
- Hackman, T., Mantere, M. J., Lindborg, M., Ilyin, I., Kochukhov, O., Piskunov, N., Tuominen, I., 2012, *A&A*, 538, A126
- Hackman, T., Pelt, J., Mantere, M. J., Jetsu, L., Korhonen, H., Granzer, T., Kajatkari, P., Lehtinen, J., Strassmeier, K. G., 2013, *A&A*, 553, A40
- Jetsu, L., Pelt, J., & Tuominen, I. 1993, *A&A*, 278, 449
- Jetsu, L., Pelt, J., & Tuominen, I. 1999, *A&A*, 351, 212
- Kitchatinov, L. L. & Rüdiger, G. 1999, *A&A*, 344, 911
- Kitiashvili, I. N., Kosovichev, A. G., Wray, A. A., & Mansour, N. N., 2010, *ApJ*, 719, 307
- Kleorin, N.I., Rogachevskii, I.V., & Ruzmaikin, A.A. 1990, *Sov. Phys. JETP*, 70, 878
- Kochukhov, O., Mantere, M. J., Hackman, T., Ilyin, I., 2013, *A&A*, 550, A84
- Korhonen, H., Berdyugina, S. V., & Tuominen, I., 2004, *AN*, 325, 402
- Korhonen, H., Berdyugina, S. V., Hackman, T., Ilyin, I. V., Strassmeier, K. G. & Tuominen, I. 2007, *A&A*, 476, 881
- Küker, M. & Rüdiger, G. 1999, *A&A*, 346, 922
- Käpylä, P. J., Mantere, M. J., & Hackman, T. 2011a, *ApJ*, 742, 34
- Käpylä, P. J., Mantere, M. J., & Brandenburg, A. 2011b, *Astron. Nachr.*, 332, 833
- Käpylä, P. J., Brandenburg, A., Kleorin, N., Mantere, M. J., & Rogachevskii, I. 2012a, *MNRAS*, 422, 2465
- Käpylä, P. J., Mantere, M. J., Brandenburg, A., 2012b, *ApJL*, 755, 22
- Käpylä, P. J., Mantere, M. J., & Brandenburg, A., 2013a, *GAFD*, 107, 244
- Krause, F., & Rädler, K.-H. 1980, *Mean-field magnetohydrodynamics and dynamo theory* (Pergamon Press, Oxford)
- Lindborg, M., Korpi, M. J., Hackman, T., Tuominen, I., Ilyin, I., Piskunov, N., 2011, *A&A*, 526, A44
- Lindborg, M., Olsper, N., Pelt, J., Mantere, M. J., & Strassmeier, K. G., 2013, *A&A*, to be submitted
- Mantere, M. J., Käpylä, P. J., & Hackman, T. 2011, *Astron. Nachr.*, 332, 876
- Mitra, D., Tavakol, R., Käpylä, P. J., & Brandenburg, A., 2010, *ApJL*, 719, 1
- Moss, D., Dale, D. M., Brandenburg, A., & Tuominen I., 1995, *A&A*, 294, 155
- Moss, D., 1999, *MNRAS*, 306, 300
- Oláh, K., Korhonen, H., Kovári, Zs., Forgács-Dajka, E., & Strassmeier, K. G. 2006, *A&A*, 452, 303
- Pelt, J., Tuominen, I., & Brooke, J. 2005, *A&A*, 429, 1093
- Pelt, J., Brooke, J. M., Korpi, M. J., & Tuominen, I. 2006, *A&A*, 460, 875
- Pelt, J., Korpi, M. J., & Tuominen, I. 2010, *A&A*, 513, 48
- Pelt, J., Olsper, N., Mantere, M. J., & Tuominen, I. 2011, *A&A*, 535, 23
- Rempel, M., Schüssler, M., Cameron, R. H., & Knölker, M., 2009, *Science*, 325, 171
- Rädler, K. H., 1975, *MSRSL*, 8, 109
- Rogachevskii, I. & Kleorin, N. 2007, *Phys. Rev. E*, 76, 056307
- Stein, R. F. & Nordlund, Å, 2012, *ApJL*, 753, 13
- Tao, L., Weiss, N. O., Brownjohn, D. P., & Proctor, M. R. E., 1998, *ApJ*, 496, 39
- Tuominen, I., Berdyugina, S. V., & Korpi, M. J. 2002, *AN*, 323, 361
- Usoskin, I. G., Berdyugina, S. V., & Poutanen, J. 2005, *A&A*, 441, 347